Manometric Techniques and Tissue Metabolism, p 119, Burgess Publishing Co., Minneapolis, MN.
Wachsmuth, E. D., & Jost, J.-P. (1976) *Biochim. Biophys. Acta 437*, 454.
Wallace, R. B., Hoover, J., Barret-Connor, E., Rifkind, B. M., Hunninghake, D. B., Mackenthun, A., & Heiss, G. (1979) *Lancet 1*, 111.
Williams, D. L. (1979) *Biochemistry 18*, 1056.
Williams, D. L., Tseng, M. T., & Rottmann, W. (1978a) *Life Sci. 23*, 195.
Williams, D. L., Wang, S.-Y., & Klett, H. (1978b) *Proc. Natl. Acad. Sci. U.S.A. 75*, 5974.
Wynn, V., Doar, J. W. H., Mills, G. L., & Stokes, T. (1969) *Lancet 2*, 756.
Yamamoto, K. R., & Alberts, B. (1976) *Annu. Rev. Biochem. 45*, 721.

Fluorescence Energy Transfer on Acetylcholinesterase: Spatial Relationship between Peripheral Site and Active Center†

Harvey Alan Berman,* Juan Yguerabide, and Palmer Taylor

ABSTRACT: Spatial relationships between the peripheral site and active center on acetylcholinesterase have been examined with energy-transfer measurements by employing steady-state and time-resolved fluorescence spectroscopy. Active-center specific labeling with energy-transfer donors was accomplished with two distinct fluorescent phosphonates, the long-lived pyrenebutyl methylphosphonofluoridate and the shorter-lived (dansylamido)pentyl methylphosphonofluoridate. They react with the active-site serine of acetylcholinesterase to form fluorescent conjugates in a stoichiometry of one fluorophore per subunit. Propidium, a ligand selective for the peripheral site, serves as the energy-transfer acceptor and because it is fluorescent allows for alternative quantitation of the energy-transfer efficiency through sensitization of its emission following donor excitation. Steady-state quenching by propidium of the pyrene and dansyl conjugates occurs with 88 and 85% efficiencies, respectively. These efficiencies are in agreement with quenching values determined from analysis of the fluorescence lifetimes. The nanosecond decay rates of the conjugates measured in the absence of propidium do not display the exponential behavior observed for the free fluorophores but instead are characterized by two components. For the pyrene–enzyme conjugate two lifetimes ($\tau_1 = 80$; $\tau_2 = 160$ ns) are resolved in a ratio of amplitudes $a_1/a_2 = 3$, while for the dansyl enzyme the lifetimes ($\tau_1 = 6$; $\tau_2 = 20$ ns) are present as $a_1/a_2 = 0.33$. In the presence of propidium, the decay of the pyrene and dansyl conjugates is described by a function containing three exponential terms in which the two components having dominant amplitudes show considerably diminished lifetimes. Sensitization of acceptor fluorescence upon excitation of the pyrene donor is found to occur with only 35% efficiency compared with 85% donor quenching. The discrepancy in these values argues that propidium introduces quenching through nondipolar mechanisms as well as through excitation transfer. Maximum and minimum values for the orientation factor, K^2, were estimated from analysis of the individual donor and acceptor emission anisotropies, as well as from analysis of the transferred excitation between the pyrene–propidium pair. The intersite distance derived from examination of the pyrene–propidium pair is estimated to be $19 \leq R \leq 28$ Å, while that for the dansyl–propidium pair is $20 \leq R \leq 37$ Å. Association of bisquaternary ligands whose interquaternary distance extends 14 Å is mutually exclusive with binding of ligands at both the peripheral anionic site and the active center. Since an intersite distance exceeding 14 Å would preclude the bisquaternary ligands spanning between the sites, it is likely that a conformational change is associated with bisquaternary ligand binding. The altered conformation would either shorten the intersite distance or allosterically prevent the association of peripheral site ligands.

The 11S form of acetylcholinesterase (AchE)[1] isolated from *Torpedo* electric organs is a tetrameric enzyme composed of apparently equivalent, independent subunits of 80 000 mol wt (Taylor et al., 1974). Each subunit possesses an active center at which acetylcholine is hydrolyzed, as well as a peripheral anionic site which is spatially distinct from the active center (Changeux, 1966; Mooser & Sigman, 1974; Taylor & Lappi, 1975). Cationic ligands can alter catalysis by association at either the active center or the peripheral site, and formation of a ternary complex with active-center- and peripheral-site-selective ligands can be demonstrated. Cationic ligands that bind at the peripheral or active sites in a 1:1 stoichiometry with each subunit have been identified (Mooser & Sigman, 1974; Taylor & Lappi, 1975). Association of bisquaternary ammonium ligands of which decamethonium (I) is the prototype occurs with a 1:1 stoichiometry but is mutually exclusive with ligand association at both the active center and peripheral site (Taylor & Jacobs, 1974; Taylor & Lappi, 1975). Such an observation allows the inference that the maximum distance separating the active center and peripheral sites should be that conferred by the ten methylene carbon atoms separating the terminal cationic groups, i.e., 14 Å, a distance compatible with decamethonium spanning between the sites. In this paper steady-state and time-resolved fluorescence energy-transfer

† From the Division of Pharmacology, Department of Medicine (H.A.B. and P.T.), and Department of Biology (J.Y.), University of California, San Diego, La Jolla, California 92093. *Received September 14, 1979.* Supported in part by U.S. Public Health Service Grant GM-18360, a grant from the Muscular Dystrophy Association, and a U.S. Public Health Service award to H.A.B. (GM-5219).

[1] Abbreviations used: AchE, acetylcholinesterase; PBMPF, pyrenebutyl methylphosphonofluoridate; DC_5MPF, [1-(dimethylamino)-naphthalene-5-sulfonamido]pentyl methylphosphonofluoridate or (dansylamido)pentyl methylphosphonofluoridate; PBMP-AchE, pyrenebutyl methylphosphonoacetylcholinesterase; DC_5MP-AchE, (dansylamido)-pentyl methylphosphonoacetylcholinesterase.

0006-2960/80/0419-2226$01.00/0

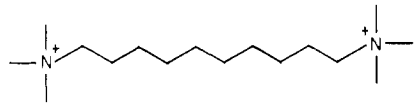

I

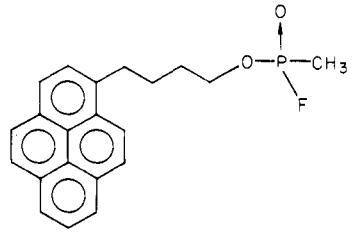

II

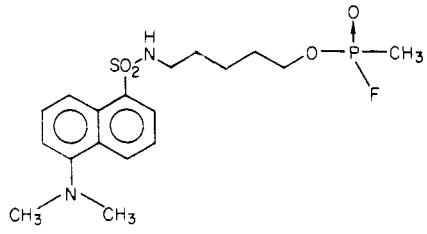

III

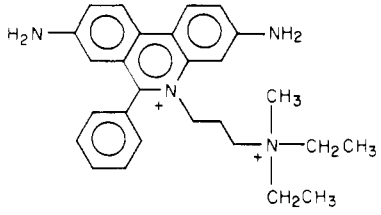

IV

measurements are employed to determine, as an independent assessment, the distance separating the peripheral site from the active center.

Pyrene (II) and dansyl (III) fluorescent phosphonate labels of the active center are employed as energy-transfer donors, and propidium (IV), which is specific for the peripheral anionic site, serves as an acceptor. The pyrene ligand, pyrenebutyl methylphosphonofluoridate (PBMPF), and the dansyl ligand, (dansylamido)pentyl methylphosphonofluoridate (DC_5MPF), react solely with the active-site serine on AchE to form the respective fluorescent conjugates PBMP–AchE and DC_5MP–AchE. They are only very slowly hydrolyzed, do not exhibit "aging", and hence are suitable for spectroscopic investigation (Berman & Taylor, 1978). Propidium presents an ideal energy-transfer acceptor since, in addition to its high affinity and selectivity for the peripheral anionic site, its fluorescence enables the efficiency of energy transfer to be determined by measuring the extent of sensitization of its emission upon excitation of the donor absorption (Taylor & Lappi, 1975).

Experimental Section

Materials. Acetylcholinesterase from *Torpedo californica* was isolated as the 11S or "lytic" species by tryptic digestion of electric organ membranes and purified to homogeneity (Taylor et al., 1974). The fluorescent phosphonylated enzyme was obtained by allowing AchE (1–10 μM) to react with a 1.5–3-fold excess of the dansyl or pyrene methylphosphonate in a 0.01 M Tris-HCl buffer, pH 8.0, containing 0.1 N NaCl and 0.04 M $MgCl_2$. After inhibition was complete (<10 min), the enzyme conjugate was separated from reactants by passage through a Sephadex G-25 column; the protein fraction in the void volume was dialyzed overnight against 2000 volumes of buffer. Stoichiometry of labeling was ascertained from the known extinction coefficient of the conjugated pyrene moiety for PBMP–AchE ($\epsilon_{348} = 3.9 \times 10^4$ M^{-1} cm^{-1}) and native AchE ($\epsilon^{280}{}_{1\%} = 17.5$) (Berman & Taylor, 1978). For the dansyl conjugate, the extinction coefficient is too low and the peak intensity too close to the protein envelope for accurate measurement. Hence, we have assumed a value of 4000 M^{-1} cm^{-1} at 335 nm for stoichiometry determinations (cf. Chen & Kernohan, 1967).

Propidium diiodide (Calbiochem), gallamine triethiodide, decamethonium chloride (K and K Chemicals), and *d*-tubocurarine (Sigma Chemical Co.) were used without further purification.

Spectroscopy. Corrected fluorescence spectra and equilibrium titrations were determined on a Farrand Mark I spectrofluorometer equipped with corrected excitation source. The emission monochromator and Hamamatsu R818 photomultiplier combination were calibrated with $BaSO_4$ (Eastman Kodak white reflectance standard) and Halon (Diano Corporation, Mansfield, MA) (Berman & Taylor, 1978). Fluorescence titrations were carried out with 1-cm^2 cuvettes positioned in the thermostated multiturreted sample compartment. Quantum yield calculations (Chen, 1965) were based on a value of 0.70 for quinine sulfate in 0.1 N H_2SO_4 (Scott et al., 1970). All fluorescence values are corrected for dilution resulting from added titrant, lamp fluctuations, and any inner-filter effects and incident scatter. UV spectra were measured on a Cary 16 spectrophotometer.

Fluorescence Lifetime Analysis. Fluorescence lifetimes were determined by the single-photon counting technique by using a modified Ortec nanosecond fluorescence spectrometer equipped with a high-pressure hydrogen arc lamp. Data accumulated in the multichannel analyzer were treated and displayed by using a PDP-11/05 computer and a Calcomp plotter. Excitation and emission bands were selected with the appropriate filters; pyrene, Corion 334 interference, 3-75 cutoff; dansyl, 7-60 interference, 3-72 cutoff. Fluorescence decay rates were resolved and assessed as either single or double exponential functions by using the method of moments. Analyses of three exponential functions were accomplished by using the method of moments with deconvolution of the lamp function when decay of dansyl fluorescence was analyzed, whereas Marquardt's nonlinear least-squares treatment (Marquardt, 1963) without deconvolution of the lamp pulse was sufficient for analysis of fluorescence lifetimes of the longer-lived pyrene moiety. The instrumental arrangement and principles of data treatment have been discussed in detail (Yguerabide, 1972).

The intensity vs. time graph, $R(t)$, directly measured with the nanosecond fluorometer is distorted by the finite duration of the lamp pulse, $L(t)$, and is related to the undistorted time course of emission $F(t)$ by the convolution integral (eq 1).

$$R(t) = \int_0^t L(T)F(t - T)\,dT \qquad (1)$$

$F(t)$ was obtained from measured graphs of $R(t)$ and $L(t)$ by deconvolution with the method of moments, assuming that $F(t)$ can be represented by the two-exponential expression

$$F(t) = a_1 e^{-t/\tau_1} + a_2 e^{-t/\tau_2} \qquad (2)$$

The deconvolution procedure yields values of a_1, a_2, τ_1, and τ_2. The time shift between $L(t)$ and $R(t)$ introduced by the spectral response properties of the detecting photomultiplier tube was corrected by using a continuously variable trombone line which allowed $L(t)$ to be shifted to the correct position in time as it was recorded. Details of this procedure are to

be described elsewhere (J. Yguerabide, unpublished experiments). Convolution of $F(t)$ so obtained with $L(T)$ generates a new function $C(t)$ which can be compared with $R(t)$. The goodness of fit is established by choosing $F(t)$ so that X^2 is a minimum

$$X^2 = \sum(C(t) - R(t))^2 \quad (3)$$

Deconvolution of $R(t)$ was performed for analysis of the dansyl fluorescence; where the pyrene emission was unperturbed and hence was far longer than the duration of the lamp spectrum, such procedures were omitted.

Energy Transfer. The efficiency (E) of energy transfer between a single donor and acceptor pair is related to the distance (R) separating the pair (Forster, 1959, 1965) (eq 4,

$$R = R_0\left(\frac{1}{E} - 1\right)^{1/6} \quad (4)$$

where R_0 represents the distance at which energy transfer is 50% efficient and is evaluated from eq 5). Q denotes the

$$R_0 = (9.765 \times 10^3)(K^2JQ\eta^{-4})^{1/6} \quad (5)$$

donor quantum yield in the absence of acceptor and η the refractive index of the medium. The overlap integral, J, represents the degree of resonance between donor and acceptor dipoles and is evaluated as the integrated mutual area of overlap between the donor emission spectrum (I_D) and the acceptor absorption spectrum (ϵ_A) (eq 6). K^2, the "orientation

$$J = \frac{\sum I_D\epsilon_A\lambda^4\Delta\lambda}{\sum I_D\Delta\lambda} \quad (6)$$

factor", accounts for the relative orientation of the donor emission and acceptor absorption dipoles during transfer and can assume a range of values between 0 and 4. Although a major uncertainty in distance measurements can be attributed to estimation of K^2, upper and lower bounds may be obtained by measurement of the rotational mobility of the donor and acceptor ligands by using fluorescence depolarization techniques as discussed later (Yguerabide, 1972, 1973; Dale & Eisinger, 1974, 1975; Dale et al., 1979).

The apparent efficiency of energy transfer was measured as the extent of quenching of the donor quantum yield or lifetime

$$E_D = 1 - \frac{I_{DA}}{I_D} \equiv 1 - \frac{\tau_{DA}}{\tau_D} \quad (7)$$

where I_{DA} and I_D are the fluorescence intensities in the presence and absence of acceptor, respectively. The respective lifetimes are denoted by τ. Where multiple lifetimes are observed, the apparent transfer efficiency in the absence of "static" components can be calculated from

$$E_D = 1 - \frac{\sum a_i\tau_i}{\sum a_i^0\tau_i^0} \quad (8)$$

The terms in the numerator and denominator denote the total fluorescence intensity for the donor in the presence and absence of acceptor, respectively, and are calculated from the experimental amplitudes (a_i) and lifetimes (τ_i). The apparent efficiency of excitation transfer equals the true efficiency only when quenching of donor fluorescence is due entirely to an excitation mechanism. The presence of other quenching mechanisms can be detected by comparing the apparent transfer efficiency determined respectively from donor quenching and sensitized acceptor fluorescence, as discussed below.

Sensitization of Acceptor Fluorescence. In those cases where the acceptor is fluorescent, another estimate of transfer efficiency is obtained from measurement of acceptor sensitization. For the case where excitation occurs at the donor wavelength and the emission is monitored at the acceptor wavelength, a simple expression for the transfer efficiency can be derived (Schiller, 1975; see Appendix):

$$E_A = \frac{OD_A}{OD_D}\left[\frac{I_{AD}}{I_A} - 1\right] \quad (9)$$

where I_{AD} and I_A are the emission intensities of the acceptor in the presence and absence of donor, respectively, and OD_D and OD_A are the optical densities at the donor-excitation wavelength of the enzyme-bound donor and acceptor, respectively. Simultaneous excitation of acceptor directly and through transfer from the donor is accounted for in this equation.

Orientation Factor, K^2. The interaction between two electric dipoles depends on their relative spatial orientation as expressed by the equation for the orientation factor, K^2 (eq 10), where

$$K^2 = (\cos\theta_T - 3\cos\theta_D\cos\theta_A)^2 \quad (10)$$

θ_T denotes the angle between the donor-emission and acceptor-absorption dipoles and θ_D and θ_A represent the angles between the respective moments and the vector adjoining D and A. Individual depolarizing events influence the measured emission anisotropy, r, as expressed by Soleillet's theorem (cf. Dale & Eisinger, 1975; Dale et al., 1979)

$$r = 0.4\prod_i d_i \quad (11)$$

where d_i denotes the observed depolarizing factor by which the transition moment is altered during each depolarizing event and 0.4 represents the fundamental limiting anisotropy assuming that the emission and absorption moments remain coincident after the absorption of radiation. For the case where D and A reorient in an axially symmetric manner, the *observed* depolarizing factor $\langle d\rangle$ can be related to a donor or acceptor *axial* depolarizing factor, $\langle d_{D,A}{}^x\rangle$ (eq 12). In the dynamic

$$\frac{r_{D,A}}{0.4} = \langle d_{D,A}\rangle = \langle d_{D,A}{}^x\rangle \quad (12)$$

limit where all possible orientations are explored during transfer, the *measured* (average) transfer depolarizing factor, $\langle d_T\rangle$, is represented by the product of three depolarizing factors corresponding to events associated with the individual donor, $\langle d_D{}^x\rangle$, and acceptor, $\langle d_A{}^x\rangle$, and with the donor–acceptor pair (eq 13). $\langle d_T\rangle$ represents the dynamically averaged depo-

$$\langle d_T\rangle = \langle d_D{}^x\rangle d_T{}^x\langle d_A{}^x\rangle \quad (13)$$

larizing factor measured for the transferred excitation, while $d_T{}^x$, the *axial* transfer depolarizing factor, is related to the angle between the axes of the D and A distribution of position moments (Dale et al., 1979).

Knowledge of $\langle d_D{}^x\rangle$ and $\langle d_A{}^x\rangle$, obtained from analysis of the fluorescence depolarization of D and A individually, and $\langle d_T\rangle$, obtained from measurement of polarized excitation transferred between the D–A pair, affords information on the angles which determine K^2 and hence the limiting values of K^2. In the absence of information on the polarization of transferred excitation, limits on K^2 may be estimated, although with greater uncertainty, from analysis solely of the limiting emission anisotropies of D and A (Dale & Eisinger, 1975; Dale et al., 1979).

Results

Donor and Acceptor Spectra. The absorption spectrum of propidium bound to AchE overlaps the fluorescence spectra of the conjugated pyrene and dansyl moieties of PBMP–AchE

Table I: Energy-Transfer Parameters for Donor-Propidium Pairs on Acetylcholinesterase

donor	Q^a	J (cm^6/mol)	K^2	R_0 (Å)^b	E	R (Å)	$R_{2/3}{}^e$ (Å)
pyrenebutyl	0.3	8.4×10^{-15}	0.25–2.2	22.8–32.8	0.74^d	19–28	23
(dansylamido)pentyl	0.78	2.6×10^{-14}	0.08–3.2	26.7–49.5	0.85^c	20–37	28.5

[a] Quantum yields are based on a value of 0.70 for quinine (Scott et al., 1970). [b] Calculated from eq 5. [c] Donor quenching efficiency computed from eq 7. [d] Dipolar transfer efficiency computed by using eq 14 and employing $E_A = 35\%$ and $E_D = 88\%$. [e] Distance calculated by employing $K^2 = 2/3$.

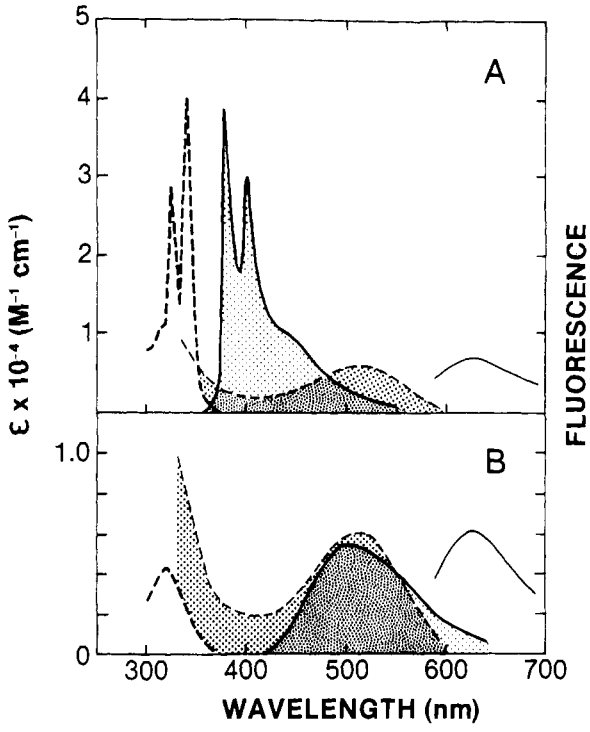

FIGURE 1: Spectral relationships characterizing donor–propidium energy-transfer pairs on acetylcholinesterase. The relationships for the pyrenebutyl conjugate, PBMP-AchE (A), and the (dansylamido)pentyl conjugate, DC_5MP-AchE (B), and complexed propidium are illustrated. The absorption (---) and emission (—) spectra for the donor are drawn with heavier lines than for the acceptor. In addition, the darkest tone serves to emphasize the region of overlap between the donor emission (light tone) and acceptor absorption (dark tone) spectra. The absorption spectra are presented as extinction coefficients (M^{-1} cm^{-1}) while the corrected emission spectra are presented in arbitrary intensity units and are not shown in proportion to the relative quantum yields of donor and acceptor.

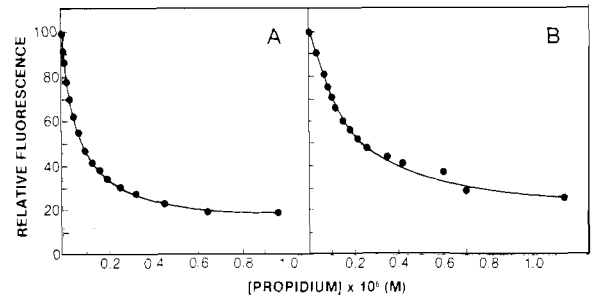

FIGURE 2: Fluorescence titrations with propidium of the pyrenebutyl methylphosphono- and (dansylamido)pentyl methylphosphono-acetylcholinesterases. (A) Fluorescence quenching of the pyrene donor of PBMP-AchE (1×10^{-7} M) upon titration with propidium. The excitation and emission wavelengths were 348 and 400 nm, respectively. (B) Fluorescence quenching of the dansyl donor of DC_5MP-AchE (2×10^{-7} M) upon titration with propidium. The excitation and emission wavelengths were 335 and 500 nm, respectively. In both titrations low-ionic-strength buffer (1 mM Tris-HCl, pH 8.0) was employed. From the slopes of Scatchard plots we calculate the propidium dissociation constant for the phosphonylated enzymes to be 1×10^{-7} M, which is in substantial agreement with the value found for the native species.

and DC_5MP–AchE. The spectral relationships for the donor–acceptor pairs are shown in Figure 1 and the calculated overlap integrals are presented in Table I. The spectral overlap, quantum yields in the absence of acceptor, and consequently the critical transfer distances R_0 characterizing the pyrene and dansyl phosphonates exhibit distinct differences. Hence, use of these two donors of different spectroscopic character should serve as independent measures of distance. Efficiencies of energy transfer between excited-state dipoles were determined by measuring the quenching of donor fluorescence, reduction in donor lifetimes, and sensitization of fluorescence of the acceptor, propidium.

Donor Quenching. Fluorescence of the pyrene and dansyl moieties of the respective phosphonate conjugates is diminished in the presence of propidium. The titration profile of PBMP–AchE in the presence of varying concentrations of propidium (Figure 2A) exhibits a simple, saturable, binding isotherm indicative of site-specific propidium binding. At saturation, pyrene fluorescence is quenched to ~12% of its original intensity, a value which corresponds to an apparent transfer efficiency of 88 ± 4%. In similar fashion, propidium titration of the dansyl conjugate shows a saturable binding profile from which we calculate an apparent transfer efficiency of 85 ± 3% (Figure 2B). Scatchard plots of these data give calculated dissociation constants of $\sim 1 \times 10^{-7}$ M in 1 mM Tris-HCl buffer (pH 8.0). The propidium dissociation constant calculated from the energy-transfer titrations is in reasonable agreement with that found for the native enzyme and indicates that phosphonylation of the active center does not appreciably alter the interaction of propidium with AchE. Furthermore, the extent of pyrene quenching by propidium is independent of the ionic strength of the buffer since an equivalent transfer efficiency was observed in 0.01 M Tris-HCl buffer containing 0.1 N NaCl and 0.04 M $MgCl_2$ (Berman & Taylor, 1978).

Dissociation of propidium by the peripheral-site ligands that lack spectral overlap with the pyrene or dansyl moieties effects a restoration of donor fluorescence; however, the fluorescence of the complexes formed from back titration is not identical with that of PBMP–AchE and DC_5MP–AchE in the absence of associated peripheral-site ligand (Epstein et al., 1979; H. A. Berman, unpublished experiments).

Nanosecond Lifetime Determinations. Fluorescence decay rates of the unconjugated pyrenebutyl methylphosphonofluoridate in solutions of glycerol–H_2O (90:10) and the corresponding dansyl phosphonate in ethanol obey exponential behavior for which the respective lifetimes are calculated to be 150 and 14 ns. Corresponding fluorescence decay rates of PBMP–AchE (Figure 3A) and DC_5MP–AchE (Figure 3B), in contrast, do not display monoexponential behavior and are more adequately described by equations containing two exponential terms (eq 2). Fluorescence decay of the pyrene–AchE conjugate is characterized by two lifetimes ($\tau_1 = 80$, $\tau_2 = 160$ ns) for which the ratio of respective amplitudes is $a_1/a_2 = 3$. The temporal emission of the dansyl conjugate also occurs with two components ($\tau_1 = 6$, $\tau_2 = 20$ ns) for which the ratio of amplitudes is $a_1/a_2 = 0.33$ (Table II). The

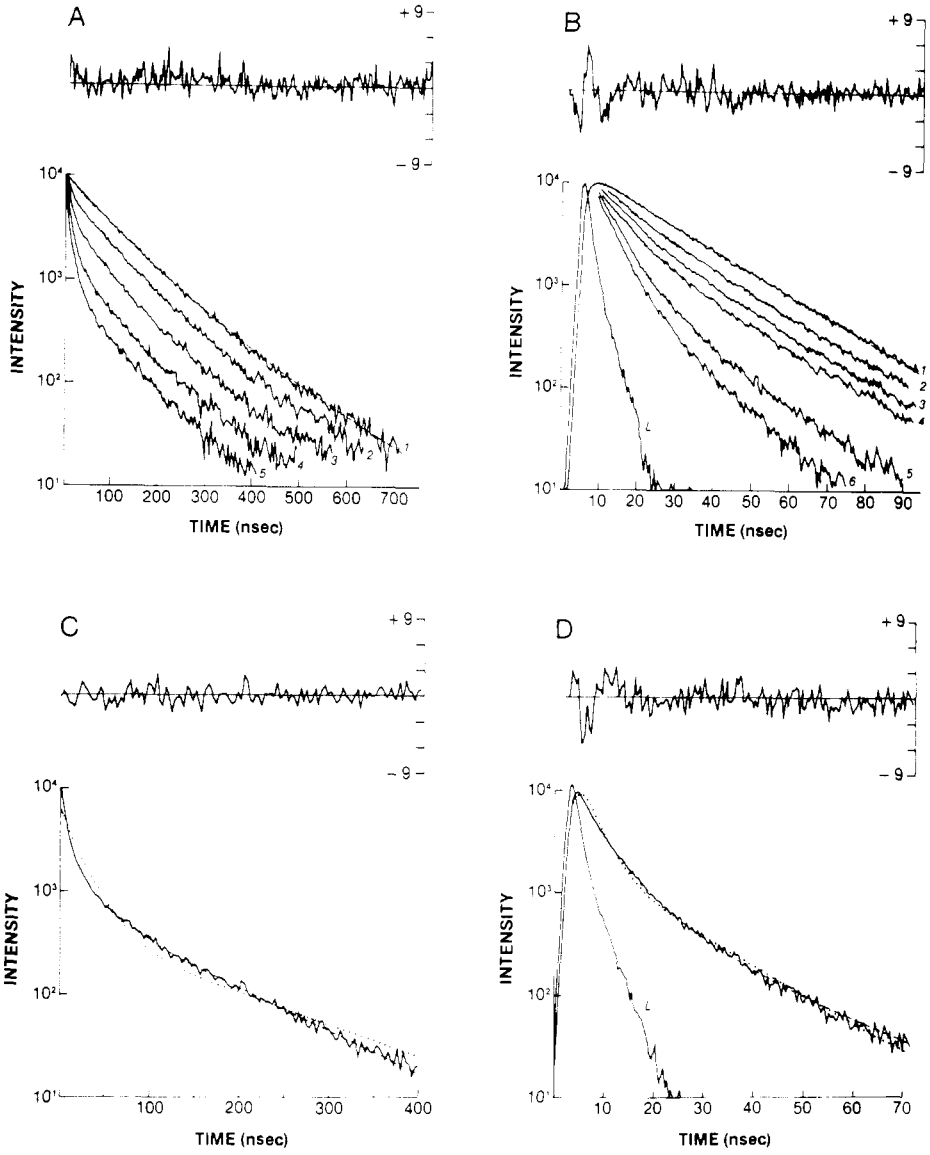

FIGURE 3: Nanosecond fluorescence decay rates of the pyrenebutyl and (dansylamido)pentyl methylphosphonoacetylcholinesterases in the presence and absence of propidium. Typical experiments for lifetime quenching required the presence of enzyme at concentrations greater than 1×10^{-6} M. The extent of saturation of propidium sites was calculated from its dissociation constant, $K_D = 1 \times 10^{-7}$ M. The medium was 1 mM Tris-HCl buffer, pH 8. During the titrations with propidium, the pulse frequency (30 kHz) of the H_2 arc lamp varied less than 3%. (A) Fluorescence decay of PBMP-AchE in the presence and absence of propidium. Curve 1 represents the pyrene decay in the absence of propidium; deviation of the experimental curve (—) from a theoretical fit (- - -) comprising a two-exponential function is shown in the upper curve. Curves 2–5 represent the pyrene decay in the presence of different concentrations of propidium where the acceptor sites were complexed to 37, 53, 89, and 98% saturation, respectively. (B) Fluorescence decay of DC_5MP-AchE in the presence and absence of propidium. Curve 1 represents the dansyl decay measured in the absence of propidium. Deviation of the experimental (—) from a two-exponential theoretical function (- - -) is shown in the upper trace. Curves 2–6 show the dansyl decay in the presence of different concentrations of propidium where the acceptor sites were complexed to 54, 68, 80, 96, and 98% saturation, respectively. (C) Comparison of two- and three-exponential curve fits with experimental data for PBMP-AchE in the presence of propidium. Acceptor sites were complexed to 95% saturation. The deviation of the three-exponential fit (- - -) from the experimental data is shown in the upper trace; $X^2/N = 0.82$. The fit to a two-exponential function (···) shows a deviation ~30% from the experimental value at the peak intensity; $X^2/N = 27$. (D) Comparison of two- and three-exponential curve fits with experimental data for DC_5MP-AchE in the presence of propidium. Acceptor sites were complexed to 98% saturation. The deviation of the three-exponential function (- - -) from the experimental data is shown in the upper trace; $X^2/N = 4$. The curve fit to a two-exponential function (···) gives $X^2/N = 15.6$.

occurrence of more than a single lifetime likely reflects multiple orientations of an intrinsically flexible ligand.

In the presence of propidium, the lifetimes and respective amplitudes of PBMP–AchE and DC_5MP–AchE are dramatically altered. A comparison of the two- and three-exponential-curve fits for the pyrene and dansyl conjugates in the presence of propidium illustrates the superior description of the experimental data by a three-exponential function as measured by the deviation over the duration of measurement (X^2/N) as well as visual inspection (Figure 3C,D; see figure legend for details). Analysis of these data with an equation containing more than two lifetimes would seem appropriate since it is necessary to account for a small fraction of donor molecules on subunits to which propidium is not bound. At concentrations of propidium approaching saturation of the binding site, the lifetime of the pyrene conjugate is reduced to 6 and 20 ns and is accompanied by a component of very small amplitude with a lifetime of ~100 ns; the ratio of amplitudes of the two short-lived components to the single long-lived component is 13. Similarly for the dansyl conjugate, the presence of propidium diminishes the excited-state lifetime to yield a dominant component comprising lifetimes of ~2

Table II: Amplitudes and Lifetimes Derived from Donor-Fluorescence Decay in the Absence and Presence of Acceptor

enzyme and ligand	amplitudes[a]			lifetimes (ns)[b]				
	a_1	a_2	a_3	τ_1	τ_2	τ_3	E_T[c]	E_{SS}[d]
PBMP-AchE	0.77	0.23		80	160			
PBMP-AchE + propidium[e]	0.77	0.16	0.07	6	21	100	85	88
DC_5MP-AchE	0.25	0.75		6	20			
DC_5MP-AchE + propidium[f]	0.71	0.26	0.03	2	5	16	81	85

[a] Relative amplitudes of the respective components; $\Sigma_i a_i = 1$. [b] Fluorescence lifetimes (ns) of the two or three resolvable components of fluorescence decay. [c] Transfer efficiency determined in the nanosecond domain with substitution of the resolved amplitudes (a_i) and lifetimes (τ_i) into eq 8. [d] Steady-state donor-quenching efficiency calculated from eq 7. [e] PBMP-AchE and propidium were present at 3.4×10^{-6} M and 16.2×10^{-6} M, respectively. From the dissociation constant for propidium in low-ionic-strength buffer, it is calculated that 98% of the enzyme sites are occupied. [f] DC_5MP-AchE and propidium were present at 6.0×10^{-6} and 22.5×10^{-6} M, respectively. From the dissociation constant for propidium in low-ionic-strength buffer, 98% of the enzyme sites are occupied.

and 5 ns and a minor component with lifetime of ~16 ns; the ratio of respective amplitudes for the two short components to the single long-lived component is 20. At high propidium concentrations the long-lived component accounts for only ~5% of the total intensity and likely reflects incomplete saturation of acceptor sites by propidium. The short-lived components of large amplitude (93–95% of the total signal) can be expected to arise from quenching of *both* microscopic populations of donor molecules which gave rise to the two lifetimes prior to complexation with propidium. Substitution into eq 8 of the amplitudes and lifetimes obtained in the presence and absence of acceptor allows calculation of 81% transfer efficiency for the dansyl conjugate and 85% transfer efficiency for the pyrene conjugate. These values obtained from the time-resolved analysis are in substantial agreement with those obtained from steady-state quenching measurements (cf. Table II).

Since the extent of lifetime quenching parallels steady-state donor quenching for the pyrene and dansyl conjugates, the donor quenching observed for PBMP–AchE, for example, should reflect 88% quenching of each donor molecule rather than 100% quenching of only 88% of the donor population. The occurrence of all-or-none quenching has been discussed for ethidium bromide quenching of the Y-base fluorescence of tRNA (Tao et al., 1970). Finally, for the dansyl conjugate the ratio of amplitudes for the two dominant components τ_1 and τ_2 changes markedly upon binding of propidium. This result is not surprising in view of our previous observation that peripheral-site ligands devoid of spectral overlap with the donor fluorophore can alter the fluorescence of DC_5MP–AchE (Epstein et al., 1979). Thus, propidium likely influences the distribution of orientations of the conjugated dansyl moiety.

Acceptor Sensitization. Sensitization of acceptor fluorescence seen upon excitation of the donor absorption band occurs with an apparent efficiency E_A which can be calculated by using eq 9. In a typical determination (Figure 4) separate cuvettes containing PBMP–AchE or native AchE at equal concentrations in low ionic strength buffer were titrated with propidium. The propidium fluorescence intensity at 625 nm was monitored upon excitation at 348 nm where the pyrene-donor extinction is maximal and is found to be 10-fold greater than that of the acceptor. Propidium emission for the pyrenebutyl phosphonylated enzyme was observed to be 3–4

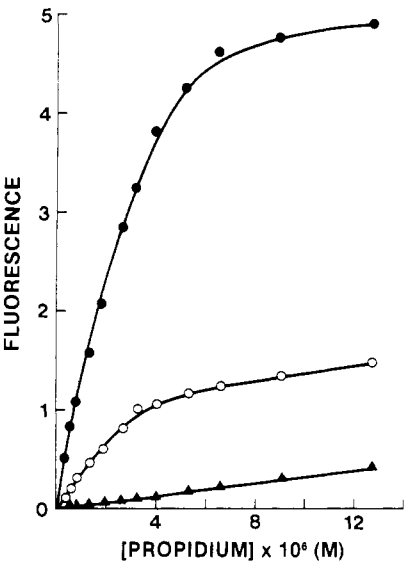

FIGURE 4: Fluorescence intensity of propidium when titrated into solutions of native and pyrenebutyl methylphosphonoacetylcholinesterase upon excitation at the wavelength of maximal donor absorption. Separate cuvettes containing equal concentrations of PBMP-AchE, native AchE, and a buffer blank were titrated with propidium. The propidium fluorescence at 625 nm was monitored upon excitation at 348 nm, where the pyrene extinction is 10-fold greater than that for propidium. (●) PBMP-AchE; (○) native AchE; (▲) buffer. The enzymes were present at concentrations of 4×10^{-6} M in 1 mM Tris-HCl, pH 8.0.

times more intense than that measured for the native enzyme. The fluorescence intensity of the propidium complex with native enzyme results from direct excitation of propidium, whereas the enhanced fluorescence of the PBMP–AchE complex reflects the additional component of energy transfer from the pyrene donor to propidium. The sensitized propidium fluorescence corresponds to a transfer efficiency of 35 ± 7% (cf. eq 9), a value which is markedly less than the efficiency determined from donor quenching.

Estimation of the Orientation Factor, K^2. Limits on the range of values for the orientation factor, K^2, were estimated from analysis of steady-state and time-resolved nanosecond measurements of donor and acceptor polarized fluorescence decay rates (see Experimental Section). For the pyrene, dansyl, and propidium ligands we measure the limiting anisotropies, A_0, to be 0.12, 0.30, and 0.33, respectively. From eq 11 and 12 these values lead to the respective observed depolarizing factors 0.30, 0.75, and 0.83, which in turn yield corresponding axial depolarizing factors of 0.55, 0.87, and 0.91.

Information on θ_T, the angle between the average orientation of the D and A transition moments, was obtained from study of the depolarization of transferred excitation between the pyrene donor and the propidium acceptor. In a typical experiment PBMP–AchE was complexed to 98% saturation with propidium. Steady-state polarization of the propidium emission at 625 nm following excitation of the pyrene donor at 348 nm was monitored in sucrose solutions of different viscosity at 22 °C (Weber, 1953; Dale & Eisinger, 1975; Dale et al., 1979). A separate cuvette containing an equal concentration of unlabeled enzyme complexed with propidium served as an adequate blank to account for direct excitation of acceptor at the excitation wavelength as well as any incident scatter.

The transferred excitation between pyrene and propidium was found to be virtually depolarized; i.e., $\langle d_T \rangle = 0$, and, hence, d_T^x, the transfer depolarizing factor also is zero (cf. eq 13). Contour maps relating $\langle d_D^x \rangle$ and $\langle d_A^x \rangle$ for the case when

$d_T^x = 0$ afford limits on the following range of values for the orientation factor characteristic of the pyrene–propidium D–A pair: $0.25 \leq K^2 \leq 2.2$ (Dale et al., 1979). In the absence of knowledge of the degree of polarization of the transferred excitation, a broader range of values is obtained for K^2 based solely on D and A anisotropies: $0.2 \leq K^2 \leq 2.7$.

For the dansyl–propidium D–A pair, estimates on K^2 were obtained solely from analysis of $\langle d_D^x \rangle$ and $\langle d_A^x \rangle$ and lead to a wide range of values for the orientation factor, $0.08 \leq K^2 \leq 3.2$.

Estimation of Distance between Peripheral and Active Sites. The computed critical transfer distances and the intersite distances are arranged in Table I. Sensitization experiments were not feasible with the dansyl conjugate since the respective extinction coefficients at the excitation wavelength highly favor absorption of light by the propidium acceptor rather than the donor (cf. Figure 1). Limits of the critical transfer distance are derived to be $23.5 \leq R_0 \leq 32.8$ Å, employing the donor quantum yield measured in the absence of acceptor and values for the orientation factor for the pyrene–propidium pair. In similar fashion for the dansyl conjugate, the critical transfer distances are calculated to be $26.7 \leq R_0 \leq 49.5$ Å (Table I).

The donor–acceptor intersite distances may now be estimated from values of R_0 and the energy-transfer efficiencies. The discrepancy, however, between 35% acceptor-sensitization and 88% donor-quenching efficiencies determined for the PBMP–AchE conjugate indicates that quenching mechanisms in addition to dipolar energy transfer prevail (Conrad & Brand, 1968; Schiller, 1975; Appendix). In such a case where E_A and E_D are found to be not equivalent, the transfer efficiency arising from the dipolar mechanism can be calculated from eq 14 (see Appendix for derivation).

$$E = \frac{E_A}{E_A - E_D + 1} \tag{14}$$

The effective dipolar transfer efficiency, E, signifies the extent of the dipolar transfer mechanism in the presence of additional transfer modes. When employed with the R_0 value calculated by using the donor quantum yield in the absence of acceptor, the value for E allows calculation of the intersite distance based solely on excitation transfer. With PBMP–AchE, for which acceptor sensitization and donor quenching have been monitored, we calculate a 74% transfer efficiency which leads to an intersite distance in the range $19 \leq R \leq 27.6$ Å. In the case of the dansyl–propidium pair, for which an 85% apparent energy-transfer efficiency is observed, we calculate the intersite distances solely on the basis of donor quenching to fall in the range $20 \leq R \leq 37$ Å. The results, including distances calculated by assuming $K^2 = 2/3$ for both D–A pairs, are summarized in Table I.

Discussion

Propidium associates with AchE at the peripheral anionic site to form a fluorescent complex characterized by a stoichiometry of one ligand/80 000-dalton subunit (Taylor & Lappi, 1975). The propidium–AchE complex dissociates in the presence of ligands selective for the peripheral but not the active site, demonstrating the topographic distinctness of the two sites. The active center in AchE for acetylcholine hydrolysis possesses a nucleophilic serine which reacts with esters of carbon, sulfur, phosphorus, and boron (Froede & Wilson, 1971; Schaffer et al., 1973; Rosenberry, 1975). By inference from substrate specificity, the catalytic serine is approximately 4.8 Å removed from an anionic locus which serves to bind the choline moiety and probably other cations as well. Since AchE does not efficiently hydrolyze butyryl and larger esters (Augustinson, 1949), the acyl pocket of the active center must be of limited dimensions.

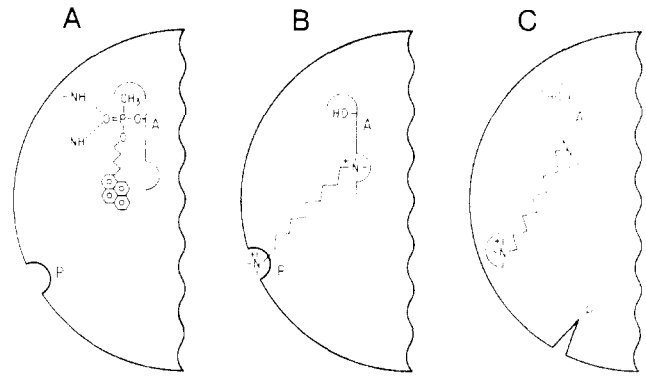

FIGURE 5: Models of a segment of a single subunit (radius = 38 Å) on acetylcholinesterase illustrating the spatial relationship between the active and peripheral sites. Panel A shows the binding orientation of the pyrenebutyl methylphosphonate ligand where rotation about the serine linkage is restricted and the pyrenebutyl moiety is oriented toward the anionic or choline binding subsite of the active center (A). The phosphonyl oxygen is stabilized through hydrogen bonding to the amide backbone hydrogens. The propidium-binding peripheral anionic site is denoted by P. Panel B illustrates the proposal for *direct* overlap between the sites of binding for decamethonium and propidium. The anionic subsite of the active center (A) serves as one locus for decamethonium while simultaneously the peripheral site (P) serves as the other and also exhibits spatial overlap with the propidium binding site. Displacement of propidium by decamethonium comes about concomitant with a conformational change involving contraction of the intersite distance between A and P. Panel C illustrates the proposed explanation of an *allosteric* influence on peripheral-site interaction. In addition to a locus at the active center (A), association of the extended end of decamethonium at a remote site acts to close down the peripheral site. Hence, spatial overlap of the respective sites is not an essential element of the proposal shown by panel C.

Phosphonylation at the active center with fluorescent phosphonates gives stable conjugates characterized by a stoichiometry of one donor molecule/80 000-dalton subunit (Berman & Taylor, 1978). Phosphonylation of the enzyme does not alter the structural integrity of the enzyme since titration of the modified protein with propidium exhibits behavior indicative of site-specific binding; in addition, active enzyme can be regenerated upon incubation of the phosphonylated enzyme with the site-directed cationic nucleophile, 2-pralidoxime.

Reaction of esters with the active-center serine to form an acyl-enzyme in the various serine esterases proceeds through formation of a tetrahedral intermediate where the carbonyl oxygen is stabilized in the "oxyanion hole" by hydrogen bonding with nitrogens of the amide backbone (Robertus et al., 1972). Since the geometry of the methyl phosphonates resembles the tetrahedral intermediate, it is to be expected that the phosphonyl oxygen is oriented in the same direction (Taylor & Jacobs, 1974). The methyl group would necessarily be situated in the spatially restricted acyl pocket which serves to orient the pyrenebutyl or (dansylamido)pentyl group toward the choline-binding anionic site (Figure 5A). This view derives support from observations on dynamic collisional quenching where pyrene fluorescence of PBMP–AchE relative to the free fluorophore is quenched preferentially by cations rather than anions (Berman & Taylor, 1978). Consequently, the intersite distance determined from energy-transfer measurements ($R > 20$ Å) represents the separation between propidium situated at the peripheral site and the pyrene or dansyl donor positioned along an axis of the active center, with the orientation of the donor group constrained to the direction of the anionic subsite (Figure 5A).

Evidence for Peripheral-Site Occupation. Simple competitive inhibition of acetylcholine hydrolysis is observed when monoquaternary ammonium cations (e.g., choline, tetramethylammonium) associate at the anionic locus of the active center (Cohen & Oosterbaan, 1963). Furthermore, *n*-alkyltrimethylammonium ions, which require a single Coulombic locus, and the corresponding bisquaternary ammonium ligands (e.g., decamethonium), which would require more than a single locus, inhibit Ach hydrolysis in a simple competitive fashion (Bergmann & Segal, 1954). The effectiveness of bisquaternary ligands of the general structure $Me_3N^+(CH_2)_nN^+Me_3$ as inhibitors of AchE increases with increasing chain length and achieves a near-maximal value at $n = 10$ (Bergmann & Segal, 1954; Paton & Zaimis, 1949) while only slight variation in maximal effectiveness is observed for $n = 12$–21 (Barlow & Zoller, 1964). Ten carbon atoms interposed between the quaternary ammonium termini correspond to an interquaternary distance of ~14 Å. The observations that structurally more complex quaternary ligands (e.g., gallamine triethiodide, *d*-tubocurarine) display partially competitive inhibition of Ach hydrolysis and that they overcome inhibition brought about by the bisquaternary but not the monoquaternary ligands indicate the participation of a binding site topographically distinct from the active center (Changeux, 1966). Strong evidence for involvement of a peripheral anionic site is also derived from studies on the influence of bisquaternary ammonium ligands on acceleration of acylation by acyl fluorides (Belleau et al., 1970). Peak acceleration of methanesulfonylation by monoquaternary ligands was observed to occur with the *n*-hexyl ligand, whereas for bisquaternary ligands of the polymethonium series peak acceleration was observed for decamethonium. The acylation studies indicate also that the associated bisquaternary ligands do not overlap the catalytic serine residue. Moreover, bisquaternary ligands display high affinity for the alkanesulfonyl- and dialkylphosphoryl-AchE's provided the alkyl group is small (Taylor & Jacobs, 1974).

Fluorescence studies employing propidium, which is not dissociated from AchE in the presence of the active-site inhibitor, edrophonium, illustrate that the peripheral and active-center sites are spatially distinct, hence permitting formation of ternary complexes (cf. Taylor & Lappi, 1975). Moreover, despite the absence of competition with each other, both edrophonium and propidium exhibit binding profiles which are competitive with bisquaternary inhibitors possessing cationic termini separated by 14 Å (Taylor & Lappi, 1975).

The intersite distance derived from the energy-transfer measurements spans the ranges 19–28 and 20–37 Å as determined by employing the pyrene– and dansyl–propidium pairs, respectively. The overlap of intersite distances obtained by using two spectrally distinct donors should lend further significance to the measurements. The distance range for the dansyl donor, however, is based only on quenching of donor fluorescence and is subject to the potential corrections arising from the acceptor-induced alterations in the donor quantum yield by mechanisms other than dipolar energy transfer (cf. Appendix). The difference between the spectroscopic range and the 14 Å value is outside the uncertainties in the measurements and in assigning precise orientation geometries to the absorption and emission dipoles. Hence, the energy-transfer results are compelling that the spectroscopically determined distance is greater than the distance inferred from the binding of bisquaternary ligands.

Relationship between Bisquaternary Binding and Propidium Site. How can the finding that the peripheral and active-center sites are separated by greater than 20 Å accommodate the observations that decamethonium binding is mutually exclusive with association of ligands at both sites and appears to displace ligands from these loci in a competitive manner? Two alternative explanations consider that, in addition to the active-center locus for association of one quaternary group of the decamethonium molecule, binding of the extended end may come about by association at the peripheral site *directly* (Figure 5B) or at another locus which *indirectly* closes down the peripheral site (Figure 5C). The proposal for a direct influence on ligand competition (Figure 5B) predicts that upon binding of decamethonium a conformational change operates to diminish the intersite distance in the bisquaternary ligand–AchE complex. Spatial overlap of the decamethonium and propidium sites is intrinsic to this proposal. The alternative explanation (Figure 5C) proposes an allosteric influence which alters the configuration at the distant peripheral site such that binding of decamethonium precludes association of propidium. In contrast with a direct mechanism, overlap of the propidium and decamethonium sites is not required for operation of an allosteric effect.

In support of a conformational change associated with bisquaternary ligand binding, it has been observed that ligands which associate exclusively with the peripheral or active sites (e.g., propidium or *N*-methylacridinium) exhibit association rates which approach the diffusion limitation (Rosenberry & Neumann, 1977; Bolger & Taylor, 1979). Bisquaternary ligands for which the cationic termini are separated by 14 Å, in contrast, exhibit bimolecular rates that are below the diffusion-controlled rates and show, in addition to a fast step, a slow unimolecular process which is independent of the nature of the ligand (Bolger & Taylor, 1979).

The complex nature of ligand binding to the peripheral site is revealed in the finding that Ca^{2+} will antagonize association of decamethonium but not gallamine with AchE (Roufogalis & Quist, 1972), yet these two latter ligands are competitive with each other (see also Taylor & Lappi, 1975). Hence, partially distinct negative centers may be involved for the association of these ligands with the locus denoted as the peripheral anionic site. It should be recognized that the intersite distances derived from the energy-transfer measurements represent the distances characteristic of a phosphonylated enzyme after ligand association and do not necessarily represent the topographic relationship between negative subsites prior to propidium complexation.

Multiple Lifetimes. The pyrene and dansyl phosphonylated enzymes exhibit two lifetimes showing ratios of amplitudes of 3 and 0.33, respectively. Multiple lifetimes sometimes reflect labeling at heterogeneous sites, as observed typically in fluorescence studies on antibodies (Yguerabide et al., 1970; Holowka & Cathou, 1976; Lovejoy et al., 1977). Labeling on AchE at sites other than the single active site contained on each 80 000-dalton subunit seems unlikely. Upon incubation of PBMP–AchE with the nucleophile 2-pralidoxime, loss of pyrene fluorescence and the recovery of enzyme activity show close correspondence (Berman & Taylor, 1978). Moreover, if the relative amplitudes for the phosphonylated AchE species were to represent two distinct sites of labeling, then, although the respective lifetimes would be altered upon binding of propidium, the ratio of amplitudes measured in the presence and absence of propidium should be expected to be equivalent, as observed for the quenching of a heterogeneous population of tryptophanyl residues in *E. coli* DNA-binding protein (Bandyopadhyay & Wu, 1978). In the present case where a single site on AchE is labeled, the observation of multiple lifetimes likely reflects the probability for these in-

trinsically flexible ligands to achieve multiple orientations, as suggested by the temperature dependence of the amplitudes of the dansyl conjugate (H. A. Berman, unpublished experiments).

Donor Quenching and Acceptor Sensitization. The quenching efficiencies determined from measurement of steady-state fluorescence intensities agree with those determined from analysis of the corresponding nanosecond lifetimes. Quenching of the pyrene donor, however, is found to occur more efficiently than does acceptor sensitization and signifies the presence of mechanisms other than dipolar energy transfer which alter the quantum yield of the pyrene donor (Conrad & Brand, 1968; Schiller, 1975; see Appendix). The origin of such nondipolar quenching mechanisms may involve a ligand-induced conformational change that is sensed at the active center by the fluorescent phosphonate. We note that the presence of peripheral-site ligands which do not display spectral overlap with the fluorescence donors are observed to alter the pyrene emission of PBMP–AchE (H. A. Berman, unpublished experiments) and the dansyl emission of DC_5MP–AchE (Epstein et al., 1979).

Inequalities observed between donor-quenching and acceptor-sensitization studies on flexible long-chain polymers in solution have been attributed to short-range interactions between the donor and acceptor (Conrad & Brand, 1968; Schiller, 1975). The donor and acceptor sites on AchE, in contrast, constitute part of a more rigid macromolecule, for which binding at the acceptor site is expected to alter conformation at the donor site. In macromolecules containing discrete binding sites, disparities between donor quenching and acceptor sensitization may reflect allosteric alterations in the environment of the donor and acceptor sites, as we suggest for AchE. Had excitation transfer with PBMP–AchE been examined by employing a nonfluorescent acceptor or had acceptor sensitization been ignored, the intersite distance derived solely on the basis of donor quenching would have been underestimated. Comparisons between donor-quenching and acceptor-sensitization efficiencies are particularly important in energy-transfer studies on proteins where association at one site potentially influences configuration at a second site in an allosteric manner.

Appendix

Analysis of Excitation Transfer in the Presence of Nondipolar Quenching Mechanisms

When donor fluorescence quenching in the presence of acceptor occurs exclusively through a dipole-transfer mechanism, the true transfer efficiency is defined as

$$E = \frac{k_{DA}}{\frac{1}{\tau_D^0} + k_{DA}} \tag{A1}$$

where k_{DA} and τ_D^0 represent the rate of dipolar energy transfer and the donor lifetime in the absence of acceptor. Should the acceptor introduce other quenching processes in addition to quenching through an excitation-transfer mechanism, then the apparent efficiencies of donor quenching, E_D, and acceptor sensitization, E_A, will not be equivalent. To resolve such a discrepancy one may modify Forster's equations to accommodate the additional processes by introducing a reduced donor quantum yield and in turn a modified R_0 value; employment of such a critical transfer distance with E_A then allows calculation of donor–acceptor separations (Schiller, 1975). An alternative treatment, presented in this Appendix, derives an "ideal" or effective transfer efficiency which accounts for excitation transfer in the presence of nondipolar quenching modes and allows calculation of intersite distances without modification of Forster's equations.

Donor Quenching. The apparent donor-quenching efficiency in the presence of acceptor is given by equation A2. I_{DA} and

$$E_D = 1 - \frac{I_{DA}}{I_D} \tag{A2}$$

I_D represent the fluorescence intensities of the donor in the presence and absence of acceptor, respectively, and are defined mechanistically in eq A3 and A4, where n_q and OD_D represent

$$I_D = n_q(OD_D)\phi_f^D = n_q(OD_D)\frac{k_e}{k_e + k_i} \tag{A3}$$

$$I_{DA} = n_q(OD_D)\phi_f^{DA} = n_q(OD_D)\frac{k_e}{\frac{1}{\tau_D^0} + k_{DA} + k_q} \tag{A4}$$

the number of incident quanta per second and the optical density of the donor determined at the excitation wavelength, respectively. The donor quantum yield in the presence and absence of acceptor, ϕ_f^{DA} and ϕ_f^D, are defined kinetically in terms of their rates of emission, k_e, and inactivation, k_i. In the presence of A, the sum of the quenching rates other than through excitation transfer is represented by k_q. Substitution of eq A3 and A4 into A2, and rearranging terms while considering $\phi_f^D = k_e\tau_D^0$, gives the apparent donor-quenching efficiency E_D (eq A5). Note that when $k_q = 0$ the apparent

$$E_D = \frac{k_{DA} + k_q}{\frac{1}{\tau_D^0} + k_{DA} + k_q} \tag{A5}$$

donor-quenching efficiency agrees with the true efficiency (eq A1).

Acceptor Sensitization. The intensity of acceptor fluorescence upon excitation at the donor absorption band in the presence (I_{AD}) and absence (I_A) of donor is given by eq A6 and A7. Equation A7 accounts for the fluorescence intensity

$$I_A = n_q(OD_A)\phi_f^A \tag{A6}$$

$$I_{AD} = n_q(OD_A)\phi_f^A + n_q(OD_D)\phi_f^A\phi_t \tag{A7}$$

of A upon direct excitation as well as upon dipolar transfer from D; ϕ_f^A denotes the acceptor quantum yield. The transfer efficiency in the presence of additional quenching modes, ϕ_t, is defined as

$$\phi_t = \frac{k_{DA}}{\frac{1}{\tau_D^0} + k_{DA} + k_q} \tag{A8}$$

The terms OD_A and OD_D in eq A6 and A7 denote the optical densities of the acceptor and the donor, respectively, at the donor-excitation wavelength. Substitution of ϕ_t into eq A7 affords, with rearrangement, the identity:

$$\phi_t = \frac{k_{DA}}{\frac{1}{\tau_D^0} + k_{DA} + k_q} = \frac{OD_A}{OD_D}\left[\frac{I_{AD}}{I_A} - 1\right] = E_A \tag{A9}$$

The kinetically defined transfer efficiency, ϕ_t, is shown to be equal to the (apparent) acceptor sensitization efficiency, E_A, determined experimentally.

Relationship between E_D and E_A in the Presence of Multiple Quenching Modes. The equations for E_D (eq A5) and E_A (eq

A9) can be expressed as eq A10 and A11, where we define $a = k_q/k_{DA}$. Solving for a in eq A11 followed by substitution

$$E_D = \frac{1 + a}{\frac{1}{E} + a} \quad \text{(A10)}$$

$$E_A = \frac{1}{\frac{1}{E} + a} \quad \text{(A11)}$$

into eq A10 gives the dipolar transfer efficiency as we have defined it in eq A1.

$$E = \frac{E_A}{E_A - E_D + 1} = \frac{k_{DA}}{\frac{1}{\tau_D} + k_{DA}} \quad \text{(A12)}$$

The transfer efficiency E represents the efficiency that would be expected for a donor–acceptor pair if quenching mechanisms other than excitation transfer were absent. In this situation the critical transfer distance is calculated by using the donor quantum yield measured in the absence of acceptor. The term $E_A - E_D + 1$ represents the factor by which $1/\tau_D^0 + k_{DA}$ is reduced as a result of quenching mechanisms other than excitation transfer. It is noted that when E_A and E_D are equivalent, the effective transfer efficiency agrees with the value obtained from acceptor sensitization. Moreover, comparison of eq A5 and A9 illustrates that, since k_q appears in both the numerator and denominator of the expression for E_D, the influence of additional quenching modes is far greater on E_A than on E_D.

References

Augustinsson, K.-B. (1949) *Arch. Biochem. Biophys. 23*, 111–26.

Bandyopadhyay, P. K., & Wu, C.-W. (1978) *Biochemistry 17*, 4078–85.

Barlow, R. B., & Zoller, A. (1964) *Br. J. Pharmacol. 23*, 131–50.

Belleau, B., DiTullio, V., & Tsai, Y.-H. (1970) *Mol. Pharmacol. 6*, 41–5.

Bergmann, F., & Segal, R. (1954) *Biochem. J. 58*, 692–8.

Berman, H. A., & Taylor, P. (1978) *Biochemistry 17*, 1704–13.

Bolger, M. B., & Taylor, P. (1979) *Biochemistry 18*, 3622–9.

Changeux, J. P. (1966) *Mol. Pharmacol. 2*, 369–92.

Chen, R. F. (1965) *Science 150*, 1593–5.

Chen, R. F., & Kernohan, J. C. (1967) *J. Biol. Chem. 242*, 5813–23.

Cohen, J. A., & Oosterbaan, R. A. (1963) in *Handbuch der Experimentellen Pharmakologie* (Koelle, G. B., Ed.) Vol. 15, pp 299–373, Springer-Verlag, Berlin.

Conrad, R. H., & Brand, L. (1968) *Biochemistry 7*, 777–87.

Dale, R. E., & Eisinger, J. (1974) *Biopolymers 13*, 1573–1605.

Dale, R. E., & Eisinger, J. (1975) in *Biochemical Fluorescence* (Chen, R. F., & Edelhoch, H., Eds.) Vol. 1, pp 115–284, Marcel Dekker, New York.

Dale, R. E., Eisinger, J., & Blumberg, W. E. (1979) *Biophys. J. 26*, 161–94.

Epstein, D., Berman, H. A., & Taylor, P. (1979) *Biochemistry 18*, 4749–54.

Forster, Th. (1959) *Discuss. Faraday Soc. 27*, 7–17.

Forster, Th. (1965) in *Modern Quantum Chemistry* (Sinanoglu, O., Ed.) Part 3, pp 93–137, Academic Press, New York.

Froede, H. C., & Wilson, I. B. (1971) in *The Enzymes* (Boyer, P., Ed.) Vol. 5, pp 87–114, Academic Press, New York.

Holowka, D. A., & Cathou, R. E. (1976) *Biochemistry 15*, 3379–90.

Lovejoy, C., Holowka, D. A., & Cathou, R. E. (1977) *Biochemistry 16*, 3668–72.

Marquardt, D. W. (1963) *J. Soc. Ind. Appl. Math. 2*, 431–41.

Mooser, G., & Sigman, D. S. (1974) *Biochemistry 13*, 2299–307.

Paton, W. D. M., & Zàimis, E. J. (1949) *Br. J. Pharmacol. 4*, 381–400.

Robertus, J. D., Kraut, J., Alden, R. A., & Birktoft, J. J. (1972) *Biochemistry 11*, 4293–303.

Rosenberry, T. L. (1975) *Adv. Enzymol. 43*, 103–218.

Rosenberry, T. L., & Neumann, E. (1977) *Biochemistry 16*, 3870–8.

Roufogalis, B. D., & Quist, E. E. (1972) *Mol. Pharmacol. 8*, 41–9.

Schaffer, N. K., Michel, H. O., & Bridges, A. F. (1973) *Biochemistry 12*, 2946–50.

Schiller, P. W. (1975) in *Biochemical Fluorescence* (Chen, R. F., & Edelhoch, H., Eds.) Vol. 1, pp 285–303, Marcel Dekker, New York.

Scott, T. G., Spencer, R. D., Leonard, N. G., & Weber, G. (1970) *J. Am. Chem. Soc. 92*, 687–95.

Tao, T., Nelson, J. H., & Canter, C. R. (1970) *Biochemistry 9*, 3514–24.

Taylor, P., & Jacobs, N. M. (1974) *Mol. Pharmacol. 10*, 93–107.

Taylor, P., & Lappi, S. (1975) *Biochemistry 14*, 1989–97.

Taylor, P., Jones, J. W., & Jacobs, N. M. (1974) *Mol. Pharmacol. 10*, 78–92.

Weber, G. (1953) *Adv. Protein Chem. 8*, 415–59.

Yguerabide, J. (1972) *Methods Enzymol. 26*, 498–578.

Yguerabide, J. (1973) in *Fluorescence Techniques in Cell Biology* (Thaer, A. A., & Sernetz, M., Eds.) pp 311–31, Springer-Verlag, New York.

Yguerabide, J., Epstein, H. F., & Stryer, L. (1970) *J. Mol. Biol. 51*, 573–90.